

Supplementary Information for

Adaptive radiation, “taxon murk”, and the reality of early burst speciation: an example from Australia’s scincid lizards

Sonal Singhal, Ivan Prates, Huateng Huang, Maggie R. Grundler, Alan Lemmon, Emily Moriarty Lemmon, Pascal O. Title, Stephen C. Donnellan, Craig Moritz, Daniel L. Rabosky

Supplemental Tables

Table S1: The individuals included in this study ($n = 1941$), including their classification under our four taxonomies, their latitude and longitude, and accession information for double-digest restriction-site associated DNA (ddRAD) data, target capture data, and mitochondrial DNA.

Available here due to size: https://github.com/singhal/sphenophylo/blob/main/Table_S1.csv

Table S2: To the best of our knowledge, a complete listing of the studies that have used genetic data to formally evaluate species boundaries in the sphenomorphines. This is accurate as of June 2024. In total, genetic data have been used to describe 26 new species and synonymize seven others.

paper	description
(Aplin & Adams, 1998)	described a new species (<i>Ctenotus maryani</i>)
(Hutchinson & Donnellan, 1999)	described two new species (<i>Ctenotus olympicus</i> and <i>C. orientalis</i>)
(Hutchinson, Adams, & Fricker, 2006)	described elevation of two subspecies to species (<i>Ctenotus brooksi</i> and <i>C. euclae</i>)
(Smith & Adams, 2007)	described nine new species of <i>Lerista</i>
(Mecke, Doughty, & Donnellan, 2009)	described a new species (<i>Eremiascincus musivis</i>)
(Kay & Keogh, 2012)	described a new species (<i>Ctenotus ora</i>)
(Rabosky <i>et al.</i> , 2014)	described a new species (<i>Ctenotus superciliaris</i>) and synonymized six species (<i>C. borealis</i> , <i>C. brachyonyx</i> , <i>C. fallens</i> , <i>C. helenae</i> , <i>C. saxatilis</i> , <i>C. severus</i>)
(Couper, Amey, & Worthington, 2016)	described two new species (<i>Lerista hobsoni</i> and <i>L. vanderduysi</i>)
(Rabosky, Doughty, & Huang, 2017)	described two new species (<i>Ctenotus pallasotus</i> and <i>C. rhabdotus</i>)
(Amey, Couper, & Wilmer, 2019)	described two new species (<i>Lerista alia</i> and <i>L. parameles</i>)
(Hutchinson <i>et al.</i> , 2021)	described two new species (<i>Praeteropus auxilliger</i> and <i>P. monachus</i>)
(Singhal, Solis, & Rabosky, 2022)	confirmed <i>Ctenotus zastictus</i> as a distinct species
(Prates <i>et al.</i> , 2022)	described a new species (<i>Ctenotus kutjupa</i>)
(Prates, Doughty, & Rabosky, 2023b)	argued that subspecies of <i>Ctenotus pantherinus</i> subspecies are not evolutionary distinct
(Prates <i>et al.</i> , 2023a)	provided additional, genome-scale data confirming the taxonomic decisions in Rabosky <i>et al.</i> 2014
(Farquhar <i>et al.</i> , 2024)	synonymized <i>Lerista arenicola</i> with <i>L. microtis</i>

Table S3: Gamma (γ) estimates from previously-published studies, including the clade name, number of known species (richness), and number of sampled species. The summarized studies are: (Rüber & Zardoya, 2005; Kozak, Weisrock, & Larson, 2006; McKenna & Farrell, 2006; Phillipmore & Price, 2008; McPeek, 2008).

Available here due to size: https://github.com/singhal/sphenophylo/blob/main/Table_S3.csv

Supplemental Figures

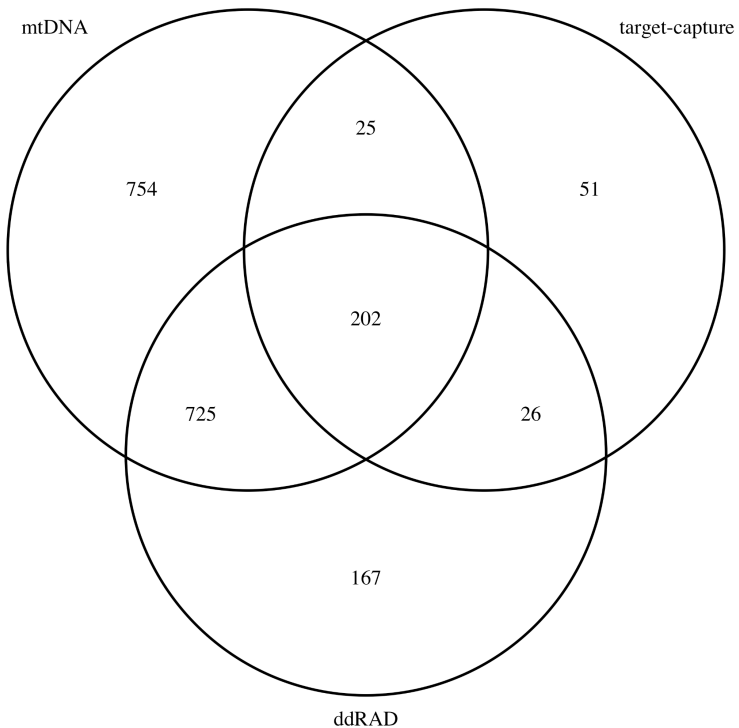


Figure S1: Distribution of marker types sampled for the 1949 ingroup and outgroup individuals included in our synthetic phylogeny. While only a small portion of individuals were sampled for all three marker types (10.4%), 50.2% individuals were sampled for at least two marker types.



Figure S2: Comparison of phylogenomic backbones inferred using a concatenated alignment with IQ-TREE2 (left) and using the coalescent-based approach implemented in ASTRAL (right). Nodes marked in red are discordant between the two topologies; 17 out of 204 nodes were discordant (8.3%). Trees are subsampled to one tip per operational species for visualization.

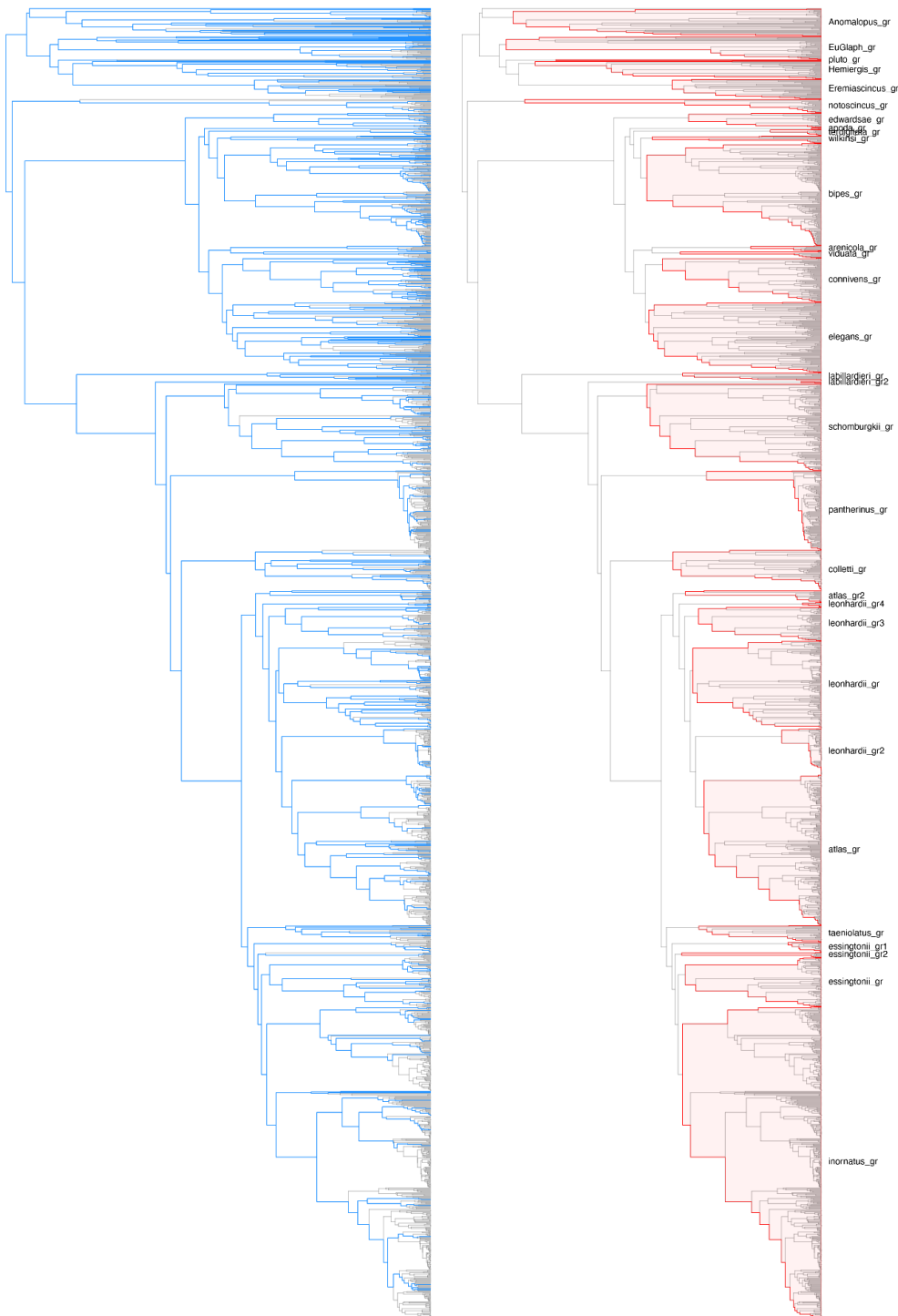


Figure S3: Constraints used in phylogenetic estimation. **(L)** Our synthetic tree with constrained edges from our phylogenomic tree in blue. **(R)** The synthetic tree split by the monophyletic groups for which we inferred local trees that were then grafted onto our phylogenomic backbone.

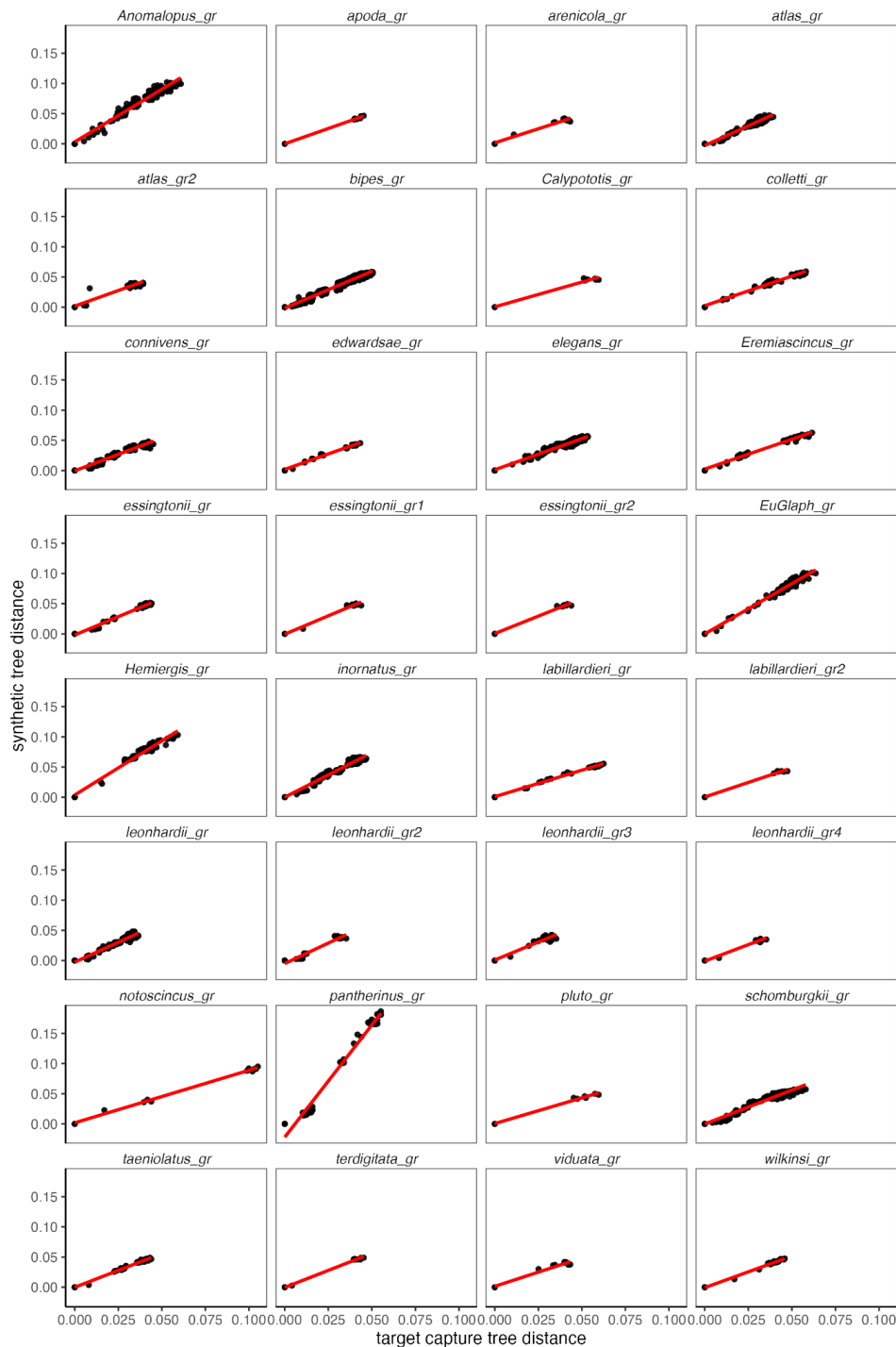


Figure S4: Correlations between phylogenetic distances estimated from phylogenomic target-capture data versus from our synthetic alignment that concatenated across all data types (SqCL, ddRAD, mtDNA). Within each of our 32 constraint groups (see Fig. S3), phylogenetic distances between the two alignments were highly correlated, and across constraint groups, the slopes were fairly similar. Average slope was 1.22 (95% range: 0.99 - 2.23). That said, we accounted for variation in slopes (e.g., *pantherinus_gr* relative to other groups) in our grafting process.

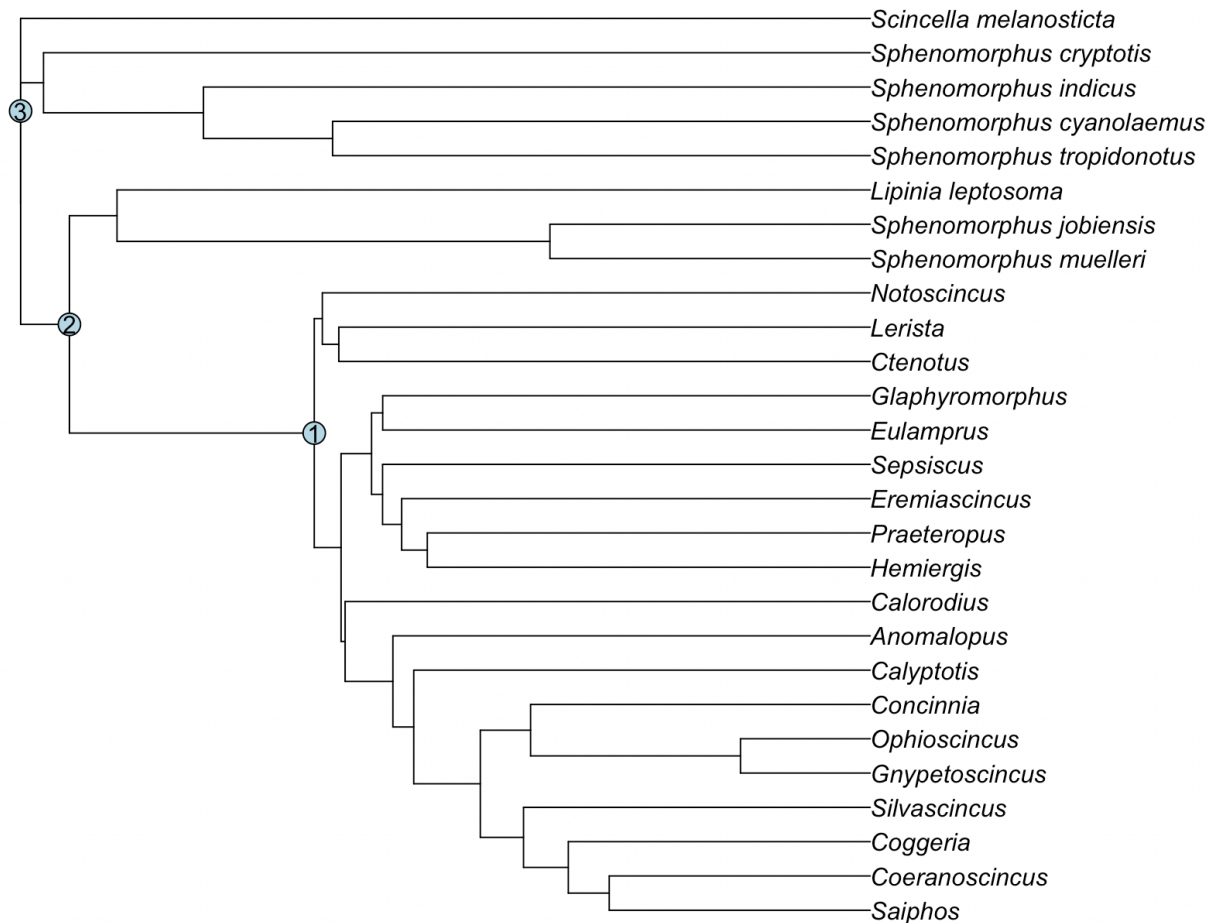
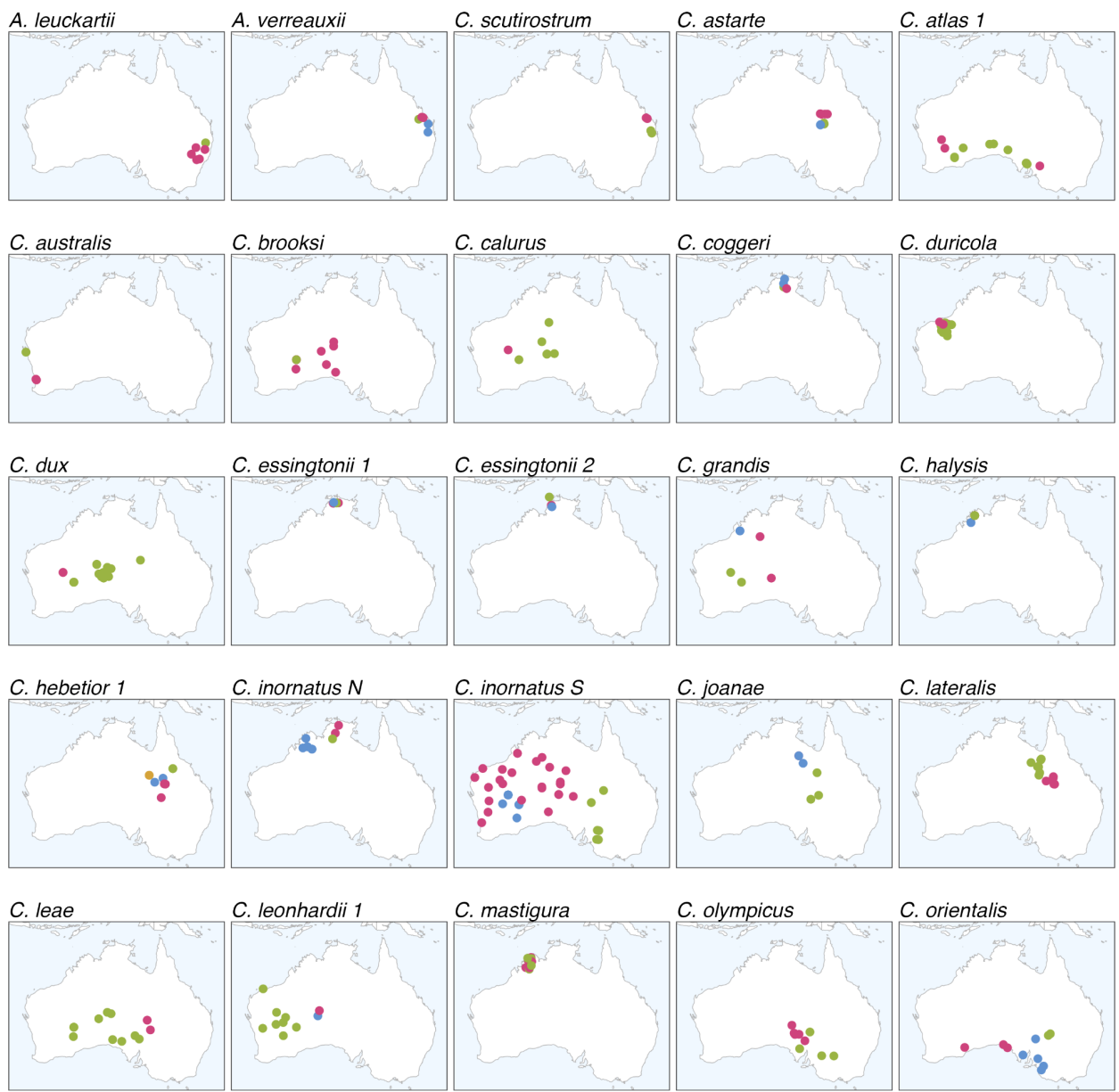
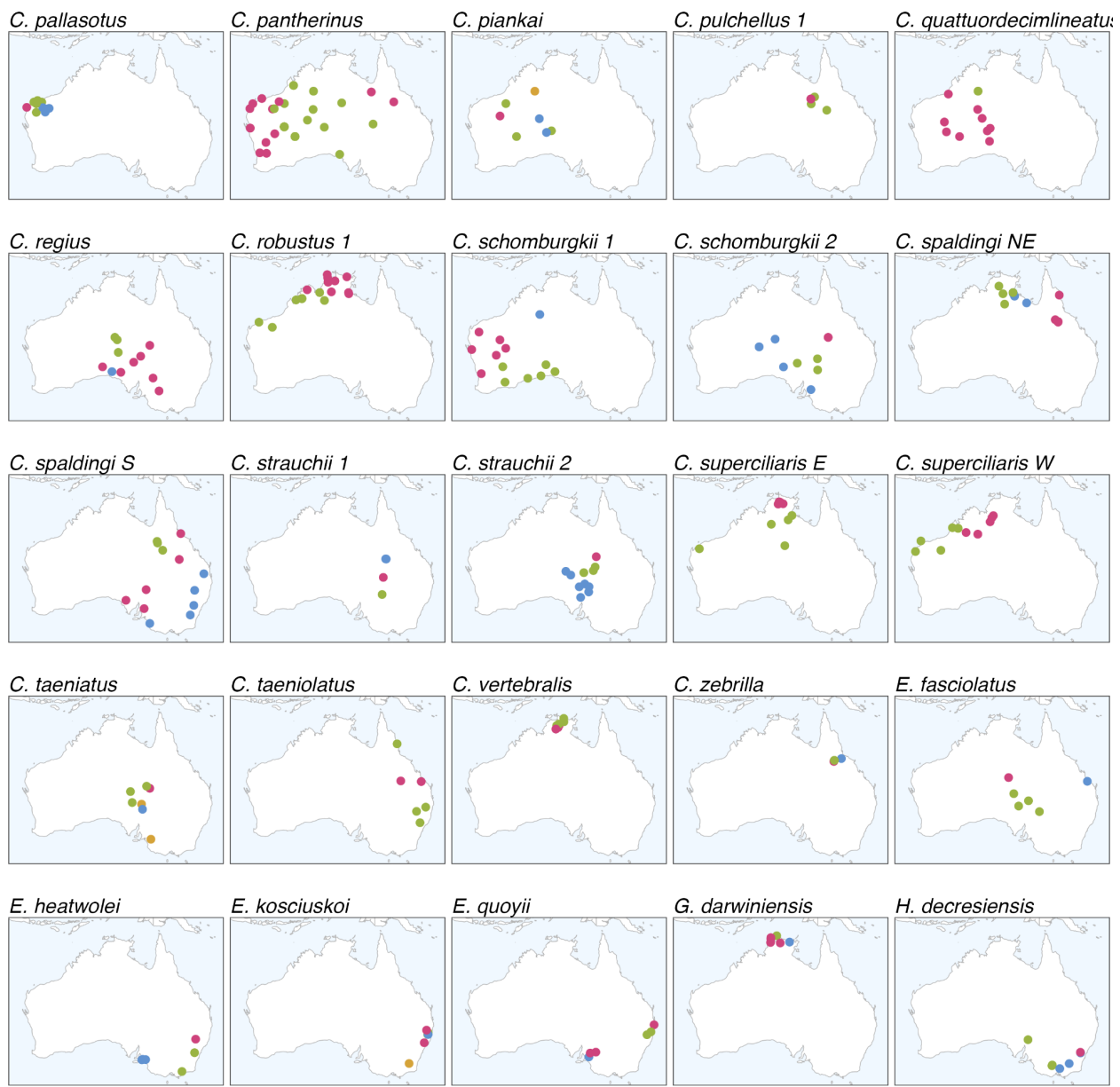
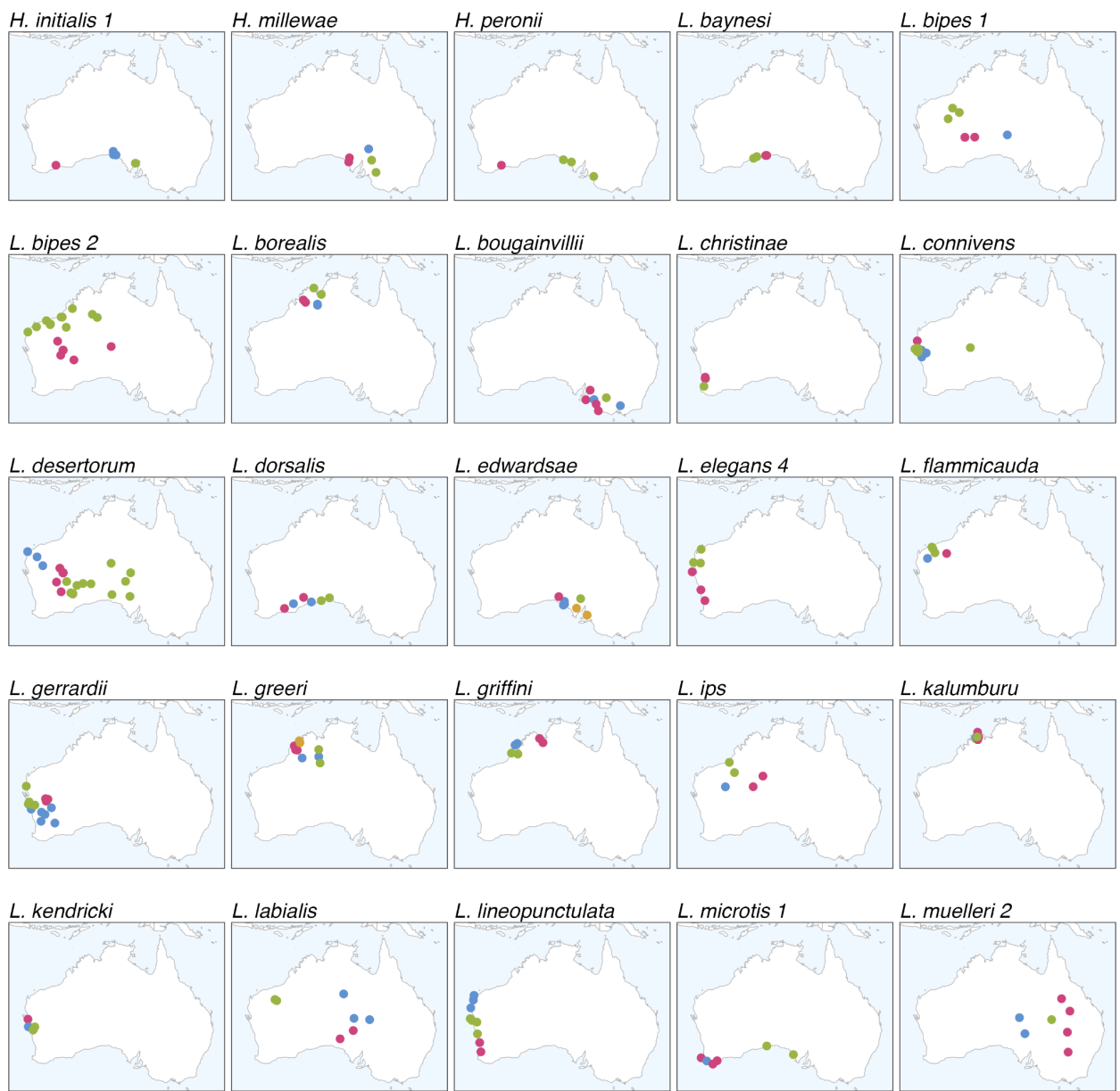


Figure S5: Our synthetic phylogeny subsampled to show one tip per ingroup genus and all eight outgroups. The three calibration points used are labeled: (1) all Australian sphenomorphines, (2) all Sahulian sphenomorphines, and (3) all sphenomorphines.







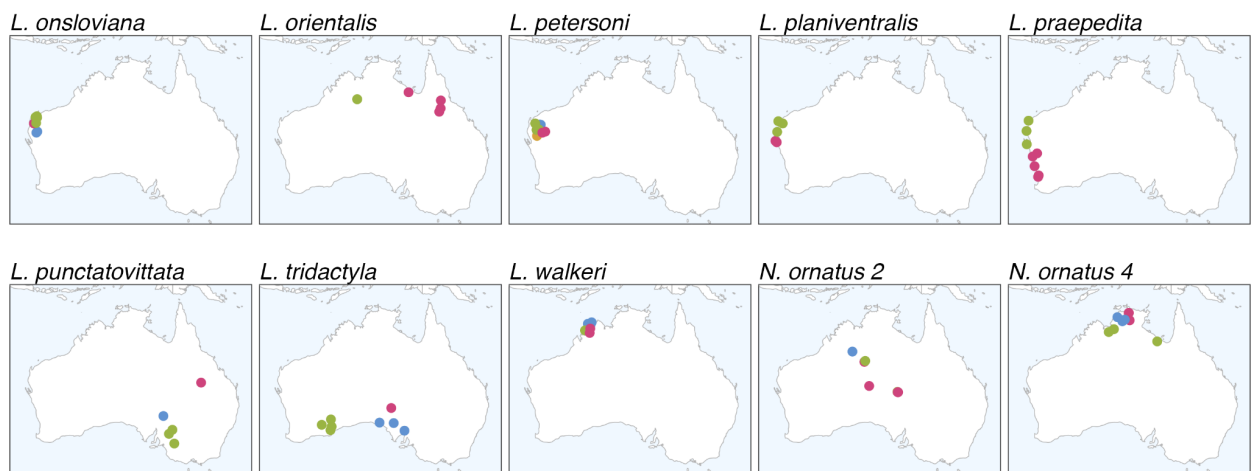


Figure S5: Maps of genetic structure identified within operational species, as inferred by fastSTRUCTURE. Each point represents an individual sampled for ddRAD data; points are colored by genetic cluster identity. Most likely number of clusters (K) was chosen using the “model components” method. These genetic clusters were treated as incipient species in our incipient taxonomy. Within-species clusters are mostly geographically circumscribed.

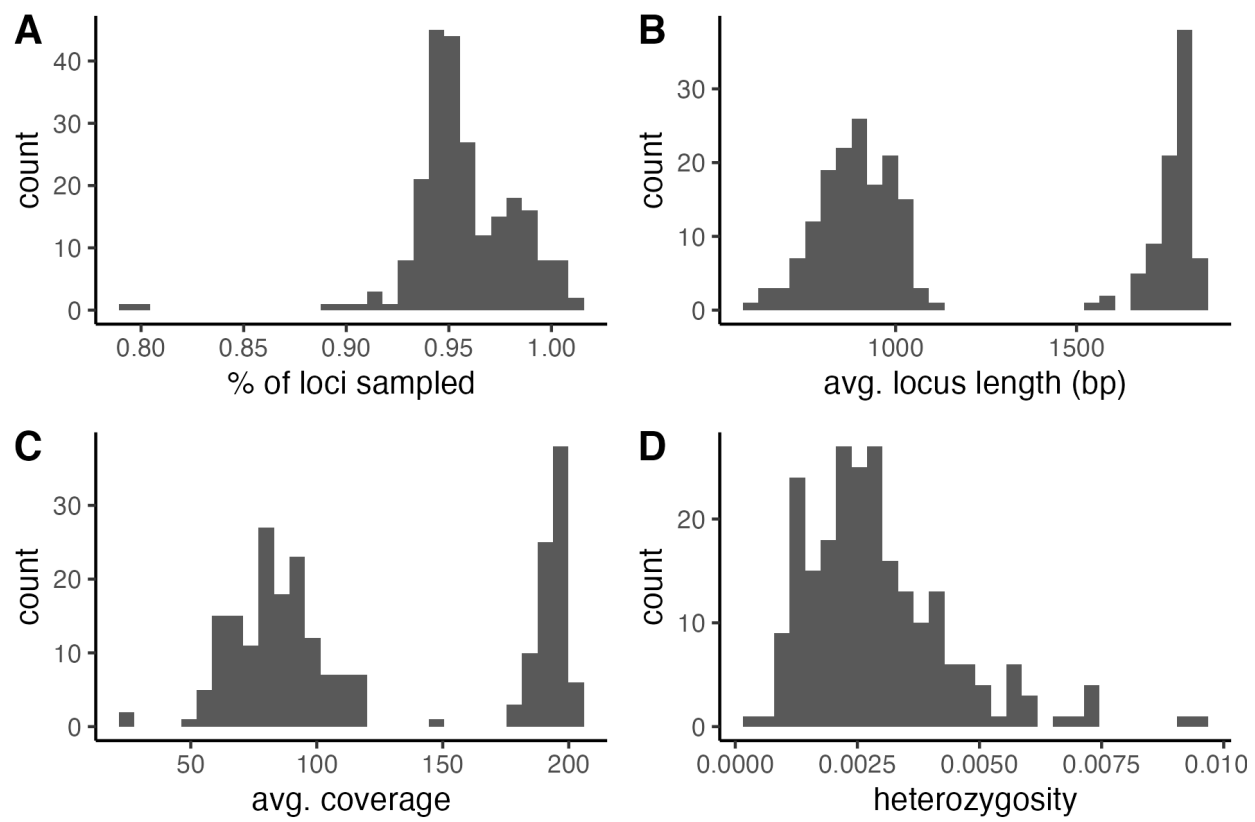


Figure S7: For the 233 individuals whose data are new to this study, our phylogenomic target capture data were uniformly high quality. They (**A**) had high levels of completeness, (**B**) recovered long loci over (**C**) high coverage and (**D**) exhibited low heterozygosity indicating contamination, barcode switching, and collapsed paralogs are unlikely. Locus length and coverage have bimodal distributions because we used two different sampling designs. Anchored hybrid enrichment (AHE) loci are longer than the average squamate conserved (SqCL) locus, and we sequenced the AHE loci to higher depth.

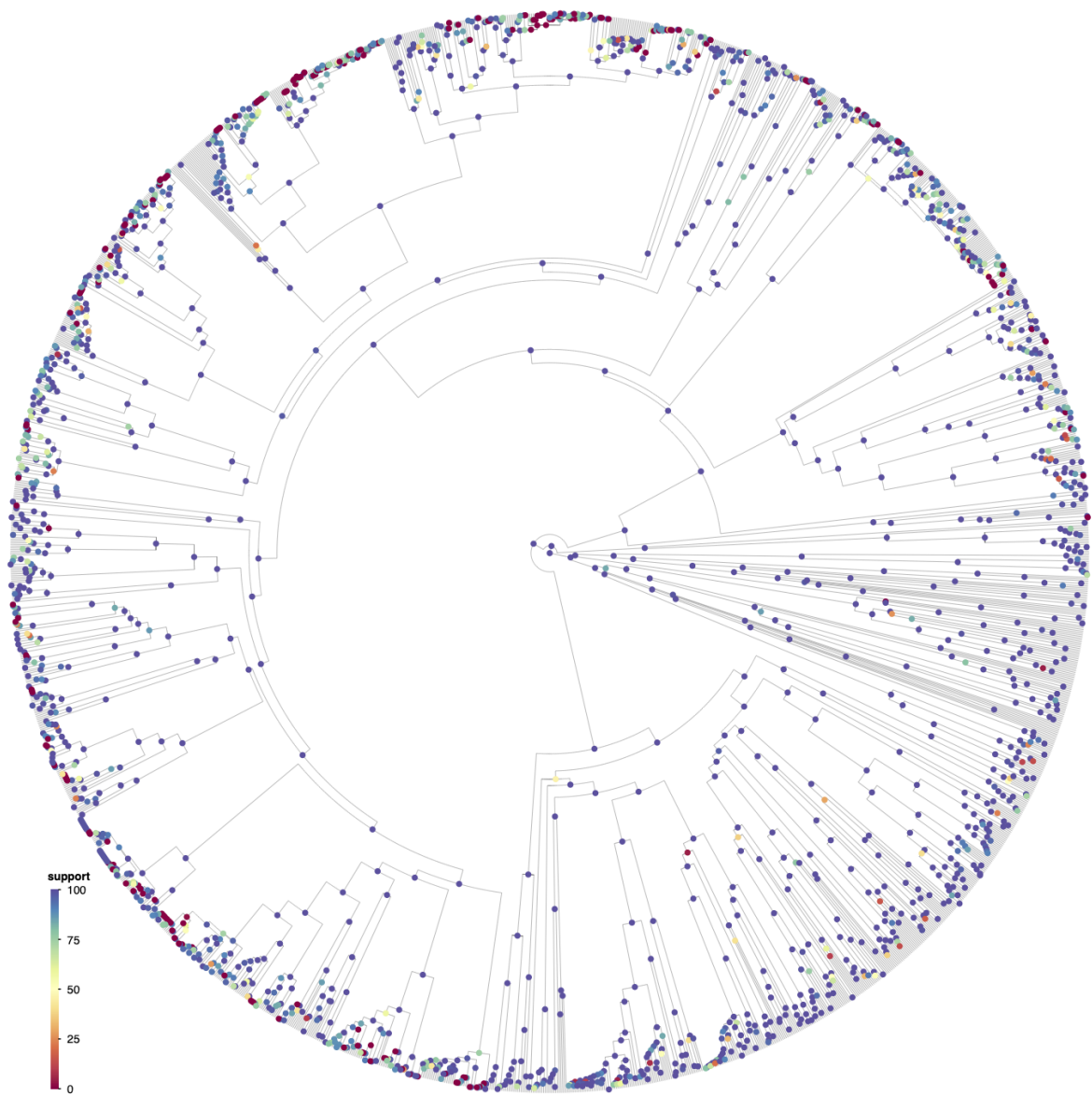


Figure S8: Topological support (as measured by Shimodaira–Hasegawa approximate likelihood ratio tests [SH-aLRT]) across the synthetic phylogeny. Most deep nodes have high support (SH-aLRT > 80); most nodes with low support are close to the tips of the tree.



Figure S9: Species-level phylogenies for the (left) operational species and (right) morphological species.

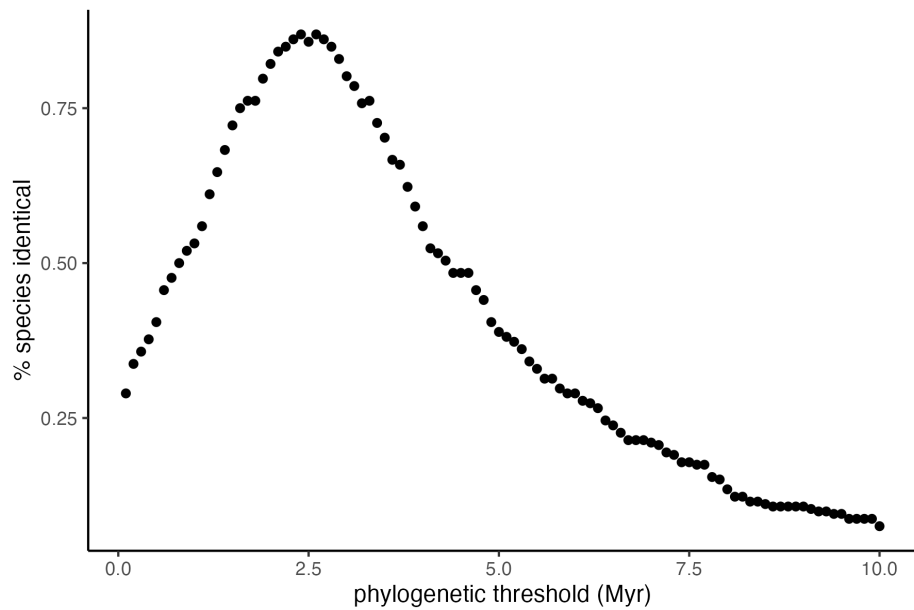


Figure S10: The reality of our operational taxonomy. We implemented our threshold taxonomy for age thresholds (τ) from 0.1 to 10 millions of years (Myr). We then determined what proportion of these units were identical to those in our operational taxonomy. Our main text presents a threshold taxonomy for $\tau = 2.5$ Myr; 87% of these threshold species are identical to an operational species.

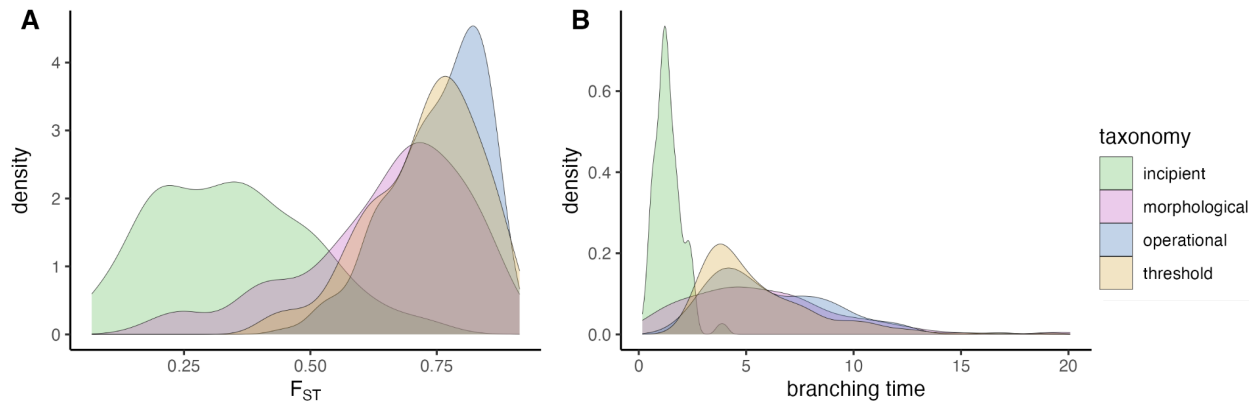


Figure S11: Patterns of divergence between sister species comparisons across our four taxonomic frameworks: morphological, operational, threshold, and incipient. We measure divergence as (A) F_{ST} and (B) branching time between comparisons. Divergence levels are similar across the morphological, operational, and threshold taxonomies; many species-level units are stable across all three of these taxonomies. Incipient species are considerably younger and have reduced genetic differentiation than species in the other frameworks.

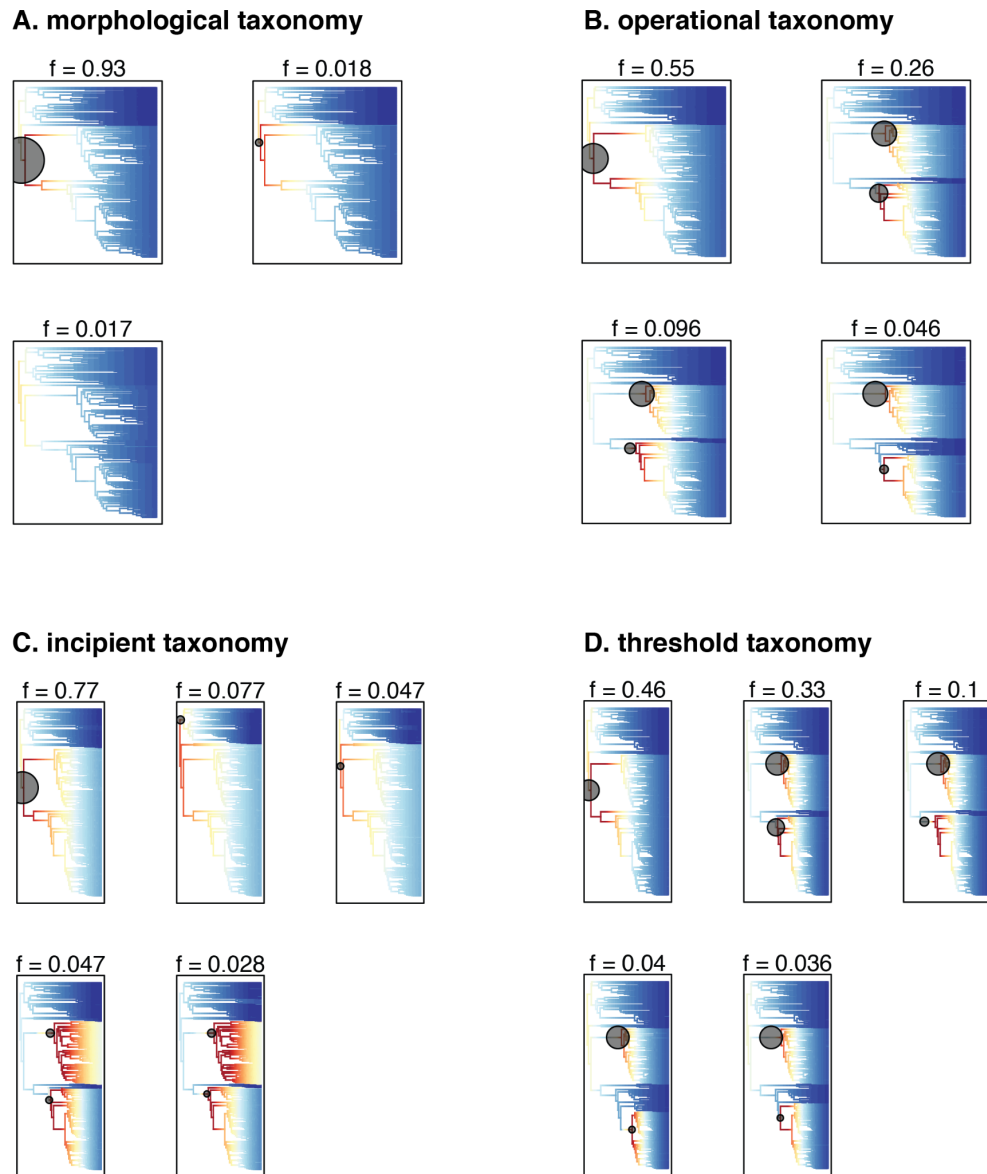


Figure S12: Credible shift set as inferred by BAMM under the **(A)** morphological, **(B)** operational, **(C)** incipient, and **(D)** threshold taxonomies. Each phylogeny shows speciation rates through time; warmer colors indicate higher speciation rates. Node circles represent the inferred location of the shift; size of the circle indicates the marginal probability that the shift occurs on that branch. Posterior probability of the shift is labeled above each plot. Under all four taxonomies, the most likely shift occurs at the base of the *Ctenotus* and *Lerista* clades, and speciation rates are high early after this shift.

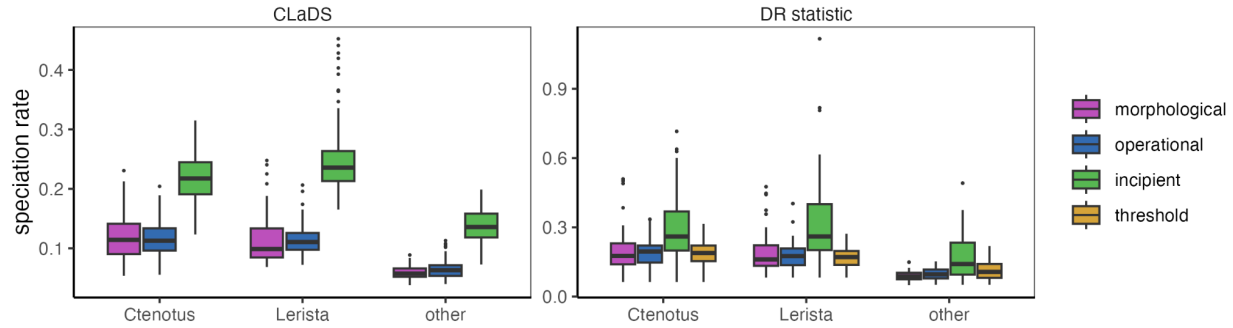


Figure S13: Speciation rates as inferred by CLaDS and the DR statistic for the morphological, operational, and incipient taxonomies. As seen with BAMM (Fig. 5F), speciation rates in *Ctenotus* and *Lerista* are nearly double that of all other genera. This result is robust across all four taxonomic frameworks.

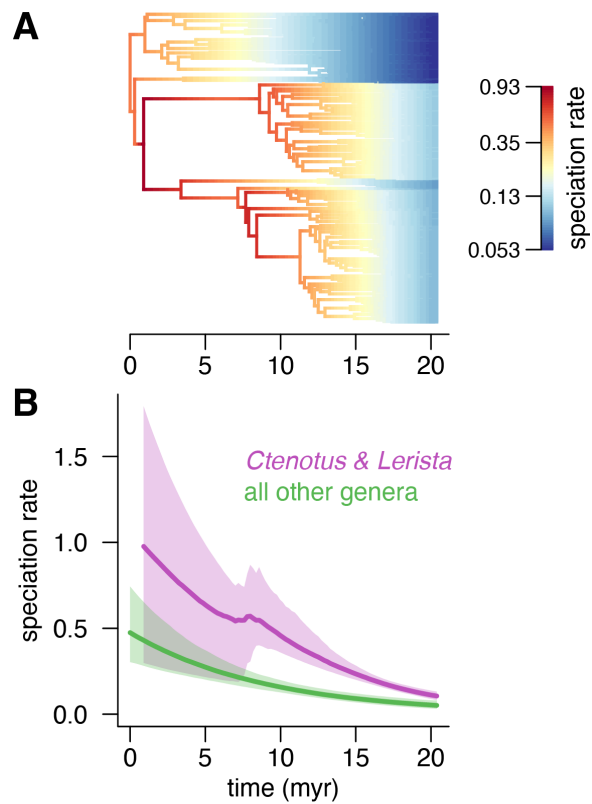


Figure S14: Slowdown in speciation rates in the sphenomorphine clade of lizards. **(A)** Reconstruction of speciation rates through time as inferred by BAMM. Color is on log-scale; warmer colors indicate higher speciation rates. **(B)** Speciation rates shown through time with their 95% confidence interval. While inferred speciation rates in *Ctenotus* and *Lerista* are double those of other genera, speciation rates across all genera are inferred to slow down through time.

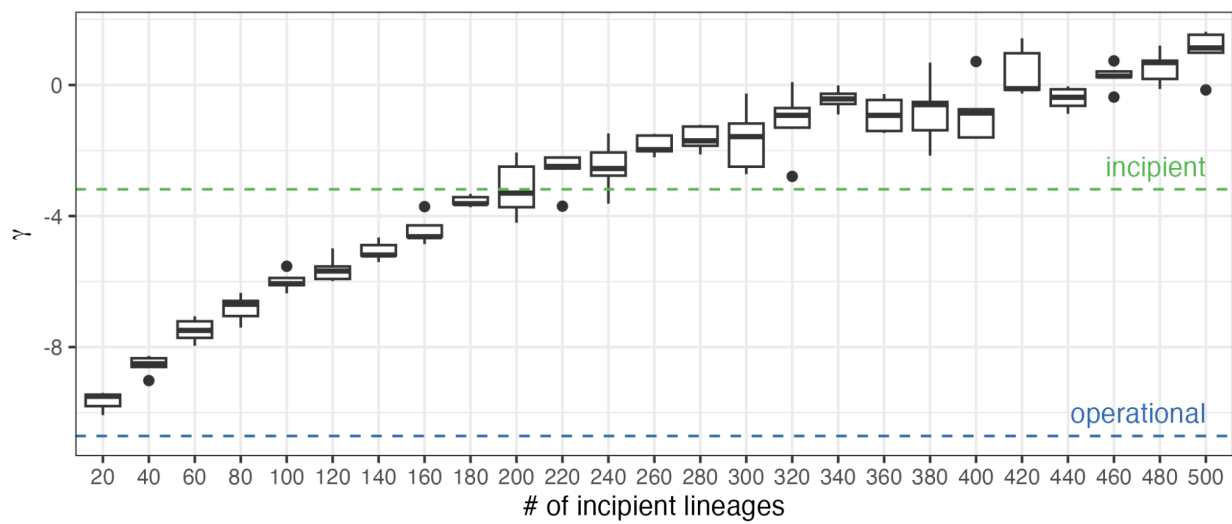


Figure S15: How adding incipient lineages to the phylogeny affects estimates of diversification slowdowns (as estimated by the gamma statistic [γ]). We simulated the addition of incipient lineages ($n = 20$ to 500) under a pure birth process to our operational taxon phylogeny ($n = 251$ tips). The dotted lines reflect the estimates of γ under our operational and incipient taxonomies. The γ value only approaches zero with the addition of upwards of 300 incipient lineages. In other words, more than half of the lineages in the clade must be “incipient lineages” before the original slowdown pattern is eroded. By comparison, our incipient taxonomy contains 151 incipient lineages.

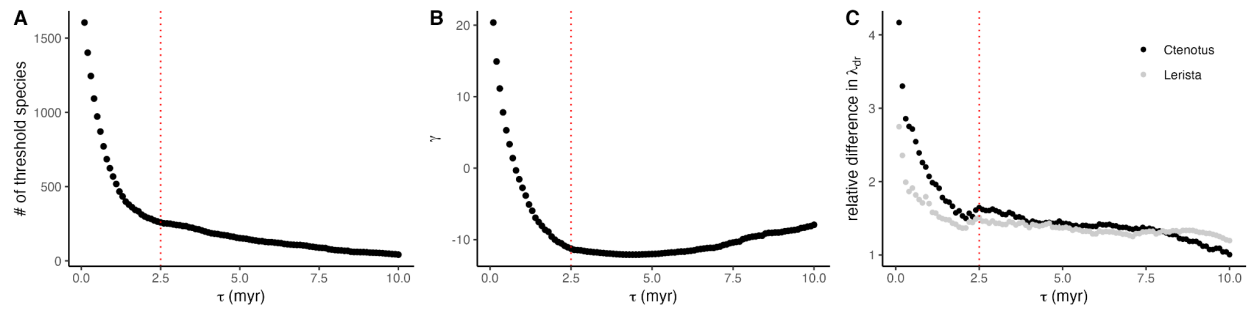


Figure S16: Diversification dynamics when species-level units are demarcated by a threshold. As the threshold (τ) in millions of years (myr) goes to 0, each tip becomes a species-level unit. **(A)** Number of species under varying τ values, **(B)** Gamma (γ) estimates across threshold taxonomies defined by varying τ values, and **(C)** relative difference in speciation rates (λ_{DR}) between *Ctenotus* species-level units (black) and *Lerista* species-level units (gray) relative to all other genera. Our main text results use a threshold of 2.5 myr (shown by the dotted red line), for which 87% of species are equivalent to those in our operational taxonomy (Fig. S10). Both of our primary diversification inferences – an increase in speciation rate in *Ctenotus* and *Lerista* & an overall, clade-wide slowdown in speciation – are robust across a fairly wide range of threshold values.

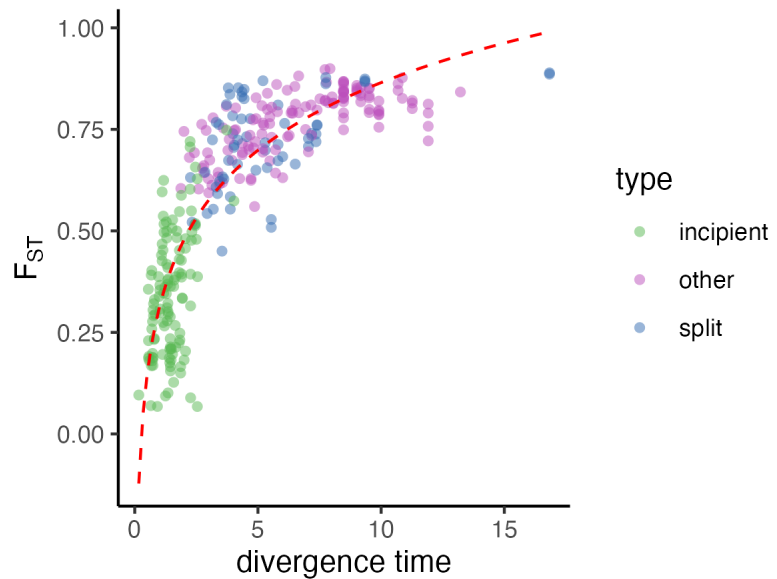


Figure S17: The relationship between F_{ST} and divergence time between sister species comparisons across both incipient and operational species. Operational species are either categorized as “split” (sister species comparison between operational species delimited from a single morphological species) or “other” (all other comparison types). Shown in red is the best-fit logarithmic curve. We see an inflection between divergence time and F_{ST} at around two million years.

Works Cited for the Supplemental Information

- Amey AP, Couper PJ & Wilmer JW. 2019.** Two new species of *Lerista* Bell, 1833 (Reptilia: Scincidae) from north Queensland populations formerly assigned to *Lerista storri* Greer, McDonald and Lawrie, 1983. *Zootaxa* **4577**: zootaxa.4577.3.3.
- Aplin KP & Adams M. 1998.** Morphological and genetic discrimination of new species and subspecies of gekkonid and scincid lizards (Squamata: Lacertilia) from the Carnarvon Basin region of Western Australia. *Journal of the Royal Society of Western Australia* **81**: 201–223.
- Couper PJ, Amey AP & Worthington WJ. 2016.** Cryptic diversity within the narrowly endemic *Lerista wilkinsi* group of north Queensland—two new species (Reptilia: Scincidae). *Zootaxa* **4162**: 61–91.
- Farquhar J, Prates I, Doughty P, Rabosky D & Chapple DG. 2024.** Morphological and genetic data challenge species and subspecies in the *Lerista microtis* group (Squamata: Scincidae). *Zootaxa* **5437**: 336–362.
- Hutchinson MN, Couper P, Amey A & Wilmer JW. 2021.** Diversity and systematics of limbless skinks (*Anomalopus*) from eastern Australia and the skeletal changes that accompany the substrate swimming body form. *Journal of herpetology* **55**.
- Hutchinson M, Adams M & Fricker S. 2006.** Genetic Variation and Taxonomy of the *Ctenotus brooksi* Species-Complex (Squamata: Scincidae). *Transactions of the Royal Society of South Australia, Incorporated. Royal Society of South Australia* **130**: 48–65.
- Hutchinson MN & Donnellan SC. 1999.** Genetic variation and taxonomy of the lizards assigned to *Ctenotus uber orientalis* Storr (Squamata: Scincidae) with description of a new species. *Records of the South Australian Museum* **32**: 173–189.
- Kay GM & Keogh JS. 2012.** Molecular phylogeny and morphological revision of the *Ctenotus labillardieri* (Reptilia: Squamata: Scincidae) species group and a new species of immediate conservation concern in the southwestern Australian biodiversity hotspot. *Zootaxa* **3390**: 1–18.
- Kozak KH, Weisrock DW & Larson A. 2006.** Rapid lineage accumulation in a non-adaptive radiation: phylogenetic analysis of diversification rates in eastern North American woodland salamanders (Plethodontidae: Plethodon). *Proceedings. Biological sciences* **273**: 539–546.
- McKenna DD & Farrell BD. 2006.** Tropical forests are both evolutionary cradles and museums of leaf beetle diversity. *Proceedings of the National Academy of Sciences of the United States of America* **103**: 10947–10951.
- McPeek MA. 2008.** The ecological dynamics of clade diversification and community assembly. *The American naturalist* **172**: E270–84.
- Mecke S, Doughty P & Donnellan SC. 2009.** A new species of *Eremiascincus* (Reptilia: Squamata: Scincidae) from the Great Sandy Desert and Pilbara Coast, Western Australia and reassignment of eight species from *Gephyromorphus* to *Eremiascincus*. *Zootaxa* **2246**: 1–20.
- Phillimore AB & Price TD. 2008.** Density-dependent cladogenesis in birds. *PLoS biology* **6**: e71.

Prates I, Hutchinson MN, Huey JA, Hillyer MJ & Rabosky DL. 2022. A new lizard species (Scincidae: *Ctenotus*) highlights persistent knowledge gaps on the biodiversity of Australia's central deserts. *Bulletin of the Society of Systematic Biologists* 1.

Prates I, Hutchinson MN, Singhal S, Moritz C & Rabosky DL. 2023a. Notes from the taxonomic disaster zone: Evolutionary drivers of intractable species boundaries in an Australian lizard clade (Scincidae: *Ctenotus*). *Molecular ecology* in press.

Prates I, Doughty P & Rabosky DL. 2023b. Subspecies at crossroads: the evolutionary significance of genomic and phenotypic variation in a wide-ranging Australian lizard (*Ctenotus pantherinus*). *Zoological journal of the Linnean Society* 197: 768–786.

Rabosky DL, Hutchinson MN, Donnellan SC, Talaba AL & Lovette IJ. 2014. Phylogenetic disassembly of species boundaries in a widespread group of Australian skinks (Scincidae: *Ctenotus*). *Molecular phylogenetics and evolution* 77: 71–82.

Rabosky DL, Doughty P & Huang H. 2017. Lizards in pinstripes: morphological and genomic evidence for two new species of scincid lizards within *Ctenotus piankai* Storr and *C. duricola* Storr (Reptilia: Scincidae) in the Australian arid zone. *Zootaxa* 4303: 1.

Rüber L & Zardoya R. 2005. Rapid cladogenesis in marine fishes revisited. *Evolution; international journal of organic evolution* 59: 1119.

Singhal S, Solis E & Rabosky DLR. 2022. World Heritage lizard: population genetics and species status of the range-restricted Hamelin skink, *Ctenotus zastictus*. *Bulletin of the Society of Systematic Biologists* 1: 8694.

Smith LA & Adams M. 2007. Revision of the *Lerista muelleri* species-group (Lacertilia: Scincidae) in Western Australia, with a redescription of *L. muelleri* (Fischer, 1881) and the description of nine new species. *RECORDS-WESTERN AUSTRALIAN MUSEUM* 23: 309.